

OPEN ACCESS

Repository of the Max Delbrück Center for Molecular Medicine (MDC) in the Helmholtz Association

<http://edoc.mdc-berlin.de/15668>

Neuromyelitis optica does not impact periventricular venous density versus healthy controls: a 7.0 Tesla MRI clinical study.

Schumacher, S., Pache, F., Bellmann-Strobl, J., Behrens, J., Dusek, P., Harms, L., Ruprecht, K., Nytrova, P., Chawla, S., Niendorf, T., Kister, I., Paul, F., Ge, Y., Wuerfel, J., Sinnecker, T.

This is the final version of the manuscript. The original article has been published in final edited form in:

Magnetic Resonance Materials in Physics, Biology and Medicine
2016 JUN ; 29(3): 535-541
[Springer Verlag](#)

© ESMRMB 2016

The final publication is available at Springer via: <http://dx.doi.org/10.1007/s10334-016-0554-3>

Neuromyelitis optica does not impact periventricular venous density versus healthy controls - a 7.0 Tesla MRI clinical study

Sophie Schumacher¹, Florence Pache, MD^{1,3}, Judith Bellmann-Strobl, MD^{1,7}, Janina Behrens, MD¹, Petr Dusek, MD^{2,3}, Lutz Harms MD^{4,5}, Klemens Ruprecht, MD^{4,5}, Petra Nytrova, MD³, Sanjeev Chawla, PhD⁸, Thoralf Niendorf, PhD^{6,7}, Ilya Kister, MD⁹, Friedemann Paul, MD^{1,4,5,7#}, Yulin Ge, MD⁸, Jens Wuerfel MD^{1,2,6,7,10*}, Tim Sinnecker, MD^{1,10,11,12*}

¹ NeuroCure Clinical Research Center, Charité – Universitätsmedizin Berlin, Germany

² Institute of Neuroradiology, Universitätsmedizin Göttingen, Germany

³ Department of Neurology and Center of Clinical Neuroscience, Charles University in Prague, 1st Faculty of Medicine and General University Hospital in Prague, Prague, Czech Republic

⁴ Clinical and Experimental Multiple Sclerosis Research Center, Charité – Universitätsmedizin Berlin, Germany

⁵ Department of Neurology, Charité – Universitätsmedizin Berlin, Germany

⁶ Berlin Ultrahigh Field Facility (B.U.F.F.), Max Delbrück Center for Molecular Medicine, Berlin, Germany

⁷ Experimental and Clinical Research Center, Charité – Universitätsmedizin Berlin and Max Delbrück Center for Molecular Medicine, Berlin, Germany

⁸ Department of Radiology, NYU School of Medicine, New York, NY, USA

⁹ Multiple Sclerosis Care Center, Department of Neurology, NYU School of Medicine, New York, NY, USA.

¹⁰ Medical Image Analysis Center AG (MIAC), Basel, Switzerland

¹¹ Department of Neurology, Asklepios Fachklinikum Teupitz, Germany

¹² Current address - Department of Neurology, Universitätsspital Basel, Switzerland

* equally contributing senior authors

Address for correspondence:

Prof. Dr. med. Friedemann Paul,

NeuroCure Clinical Research Center,

Charité -Universitätsmedizin Berlin,

Charitéplatz 1,

10117 Berlin, Germany,

Tel. +49 30 450 639705,

Fax +49 30 450 539915,

Email: friedemann.paul@charite.de

Word count abstract: 151 Word count text: 1951

Number of figures: 3 Number of tables: 1

keywords: ultrahigh field MRI, 7 Tesla MRI, multiple sclerosis, neuromyelitis optica, venous density

Acknowledgements

This work was supported by the Guthy-Jackson Charitable Foundation, the German Research Foundation (DFG Exc 257 to FP) and the German Ministry for Education and Research (Competence Network Multiple Sclerosis) to FP, FIP, JW and KR. Our technicians and study nurses Antje Els, Susan Pikol, Cynthia Kraut and Gritt Stoffels gave invaluable support.

Abstract

Object:

To quantify the periventricular venous density in neuromyelitis optica spectrum disease (NMOSD) in comparison to multiple sclerosis (MS) and healthy control subjects.

Materials and Methods:

Sixteen NMOSD, sixteen MS and sixteen healthy control subjects (HC) underwent 7.0 Tesla (7T) MRI. The imaging protocol included T_2^* weighted ($T2^*w$) fast low angle shot (FLASH) and fluid attenuated inversion recovery (FLAIR) sequences. The periventricular venous area (PVA) was manually determined by a blinded investigator in order to estimate the periventricular venous density in a region-of-interest based approach.

Results:

No significant differences in periventricular venous density indicated by PVA were detectable in NMOSD versus healthy controls ($p=0.226$). In contrast, PVA was significantly reduced in MS patients compared to HC ($p=0.013$).

Conclusion:

Unlike in MS, patients suffering from NMOSD did not show a reduced venous visibility. This finding may underscore primary and secondary pathophysiological differences between these two distinct diseases of the central nervous system.

Introduction

Neuromyelitis optica spectrum disorders (NMOSD) are often disabling neuroinflammatory, autoimmune central nervous system conditions predominantly affecting the spinal cords and optic nerves [1–4]. Prior to the discovery of a serum immunoglobulin G antibody targeting the aquaporine-4 water channel [5, 6], it was often considered a variant of multiple sclerosis (MS) as the clinical presentation of these two distinct central nervous system (CNS) diseases may overlap [1]. Indeed, patients with NMOSD are still often misdiagnosed with MS in clinical practice [7, 8].

Magnetic resonance imaging has improved our pathophysiological understanding of various CNS diseases. Driven by the improvements of gradient echo MRI techniques [9], intracranial veins can now be studied *in vivo* at 1.5 Tesla (T) and 3T, e.g. applying three dimensional (3D) susceptibility weighted imaging (SWI).

Gaining from an increased signal-to-noise ratio, increased susceptibility effects, and hence an increased sensitivity to venous deoxyhemoglobin concentration, ultrahigh field MRI at 7T advanced the visualization of even small intracranial veins [10, 11], improving the characterization of brain lesions, and facilitating the differentiation between MS and NMOSD [12, 13]. In MS, a reduced visibility of the cerebral venous system was reported recently [14, 15]. The reason for diminished visibility of the venous vasculature on 7T T2*w images in MS remains to be clarified. It may result from a reduced oxygen consumption as consequence of a widespread cerebral gliosis and hypometabolic state, leading to a reduced deoxygenation of the brain's venous blood and thus less susceptibility related signal loss on T2*w images [14, 15].

It is not known whether venous density is altered in NMOSD. Our work aimed at quantifying periventricular venous density in NMOSD including a careful comparison between healthy control subjects, NMOSD and MS patients.

Materials and Methods

Study participants

A synopsis of the demographical and clinical details is presented in Table 1. Sixteen NMOSD patients underwent ultrahigh field MRI at 7T. All NMOSD patients were seropositive for aquaporine-4-IgG. Inclusion criteria were diagnosis of NMOSD as defined by the current international consensus diagnostic criteria for NMOSD [1], age of at least 18 years, and no contraindications to 7T MRI. Sixteen patients with relapsing-remitting MS as defined by the current panel criteria [16], and sixteen age-matched healthy control subjects that were most comparable to the NMOSD cohort regarding gender, age and – if applicable - disease duration were selected from a research database of the NeuroCure Clinical Research Center (NCRC). Neurological disability was assessed with the Kurtzke Expanded Disability Status Scale (EDSS) [17]. The study was approved by the local ethics committee. Written informed consent was obtained from all subjects prior to the study.

MRI data acquisition

Ultrahigh field magnetic resonance images were acquired using a 7T whole-body MR system (Magnetom, Siemens, Erlangen, Germany) and a 24-channel RF head coil (Nova Medical, Wilmington, MA, USA).

The imaging protocol included:

- two-dimensional axial T_2^* w fast low angle shot acquisitions (FLASH; TE=25.0ms; TR=1820ms; flip angle=35°; spatial resolution=(0.5×0.5)mm², slice thickness 2mm, supratentorial brain coverage) and
- fluid attenuated inversion recovery acquisitions (FLAIR; TE=90ms; TR=16000ms; TI=2925.5ms, spatial resolution (1.0×1.0)mm², slice thickness 3mm, whole brain coverage).

Image analysis

Images were analysed using the OsiriX software package (version 3.8.1. Osirix Foundation, Genève, Switzerland) by an investigator (SS) blinded to clinical data (diagnosis, disease duration, EDSS). To estimate the periventricular venous density, we decided to use a manual approach since signal inhomogeneities on 7T T2*w images impact automated segmentation procedures. The periventricular vascular area (PVA) was assessed as described previously (Figure 1) [14]. In brief, a minimal intensity projection map (MIP) of the two adjacent axial T2*w slices that are tangential to the roof of the lateral ventricles was calculated first. This procedure eliminates the risk of double counting venous voxel in two neighbouring slices, and improves the visibility of venous structures. Next, a squared region of interest (ROI) with a length of 4cm and a width of 1cm was defined for both brain hemispheres and positioned in between the frontal and occipital horns. The investigator then manually marked each venous voxel with a signal intensity of less than 10% of the mean signal intensity of the neighbouring normal appearing vein-free white matter. The applied 10% threshold builds on previous reports [14]. To determine the mean signal intensity of the neighbouring normal appearing vein-free white matter, multiple ellipsoid ROIs with an area of 2mm² were used as a reference. Finally, the PVA (in mm²) was calculated as the sum of all venous voxel.

The left hemisphere of one MS patient was excluded from analyses due to previous brain biopsy in this area. Lesion count was conducted in a separate analysis of the FLAIR images. A lesion was defined as a hyperintensity relative to the surrounding normal-appearing white or grey matter with a diameter of at least 3mm.

Statistical analysis

All analyses were performed by using IBM SPSS Statistics (version 22, IBM, Somers, NY,

USA). P-values <0.05 were considered significant. Group differences in gender were analysed by using a Chi-squared test. Group differences in PVA and age between MS, NMOSD and healthy control subjects were assessed using a parametric Student's t-test. Normality of PVA and age was previously assessed by using a visual analysis and the Shapiro-Wilk test (PVA, p=0.931; age, p=0.188). Group differences in lesion count, time since first symptoms and EDSS were assessed by using a non-parametric Mann-Whitney U test since these variables were not normally distributed (Shapiro-Wilk, lesion count, p<0.001; time since first symptoms, p<0.001; EDSS, p=0.043). Thus, associations between lesion count and PVA were assessed using non-parametric Spearman correlation. Statistical dependencies between age and PVA were assessed using parametric Pearson correlation. Finally, gender differences in PVA were analysed by using a Mann-Whitney U test.

Results

In total, we detected 118 (mean \pm SD, range; 7 \pm 10, 0-38) cerebral FLAIR hyperintense white matter lesions in 12 of 16 NMOSD patients and 355 (mean \pm SD, range; 22 \pm 19, 0-65) cerebral white matter lesions in 15 of 16 MS patients. A total number of 112 (mean \pm SD, range; 7 \pm 13, 0-42) white matter lesions were seen in 9 of 16 healthy control subjects. These lesions in HC were non-specific in appearance and potentially related to small vessel disease in a subgroup of older healthy control subjects.

Visual inspection of 7T T2*w images shows the periventricular venous system to be altered in MS patients as compared to healthy controls. In contrast, no obvious differences were apparent when NMOSD patients were compared versus healthy control subjects. To highlight these findings Figure 2 shows T2*w images deduced from exemplary MS and NMOSD patients.

Periventricular vascular area in healthy control subjects, NMOSD and MS patients

In healthy control subjects, mean PVA was 144mm² (SD 27mm², range 92-202mm²). PVA was not associated with gender in healthy control subjects ($p=0.713$), which is in agreement with previous published results [14]. However, we observed a trend towards smaller PVA values in older healthy control subjects ($r=-0.458$, $p=0.074$).

When comparing NMOSD patients with healthy control subjects, we did not observe any differences in PVA (NMOSD, mean \pm SD, range; 133 \pm 21, 98-170 mm², $p=0.226$,) as outlined in Figure 3. In contrast, PVA was significantly reduced in MS (mean \pm SD, range; 117 \pm 30, 61-173 mm²) compared to healthy control subjects ($p=0.013$, Figure 3). There was a trend towards smaller PVA in MS versus NMOSD ($p=0.090$).

Associations with lesion count

Finally, we asked whether these differences in periventricular venous density could be due to group differences in lesion count since the periventricular venous visibility was reported

to be inversely correlated with the number of T2w lesions in MS patients.[14] Indeed, we observed an inverse correlation between the lesion count and PVA in our MS group ($r_s = -0.555$, $p=0.026$). No such an association was seen in patients with NMOSD ($r_s=0.120$, $p=0.658$).

Discussion

Increased spatial resolution and susceptibility effects of ultrahigh field MRI at 7T allow for markedly improved visualization of the brain's venous system. We have taken advantage of these capabilities to analyze the periventricular venous system in NMOSD in comparison to MS and healthy volunteers. While the periventricular venous visibility was diminished in MS compared to both NMOSD and healthy controls, there was no significant difference between venous density in NMOSD versus healthy volunteers.

To interpret our findings, one has to consider the cause of the superb visibility of venous structures in 7T T2*w or susceptibility weighted images: Deoxygenated haemoglobin is a compound with paramagnetic properties leading to susceptibility-related signal loss in gradient echo MR images. In contrast, oxygenated haemoglobin is diamagnetic. Thus, the venous visibility is highly dependent on the degree of (de-)oxygenation. Other factors, such as the velocity of the venous blood flow or the size of the venous vessel could also impact the visibility of veins on T2*w images.

Recently, various studies in MS patients identified changes in the visibility of small veins on T2*w images [14, 15]. The diminished visibility of the veins in MS may be due to a widespread cerebral hypometabolic state as a result of neurodegeneration in MS. This leads to a reduced deoxygenation of the brain's venous blood and, consequently, less susceptibility-related signal loss on T2*w images [14, 15]. This hypothesis is further supported by a quantitative MRI study that reported significantly increased venous oxygenation levels and decreased cerebral metabolic rates of oxygen in MS patients as compared with healthy controls [18]. Furthermore, vascular damage, a sequel of (perivascular) inflammation and gliosis [19] in MS, is associated with a globally reduced cerebral perfusion [20] and may thus contribute to diminished venous visibility on T2*w images [14, 15]. Another possible cause of decreased oxygen uptake is the high level of

nitric oxide (NO) due to repetitive vascular inflammation in MS competitively inhibiting mitochondrial uptake of oxygen in MS [18].

In contradistinction to MS, venous density in NMOSD patients was found to be similar to that in healthy controls. The comprehensive interpretation of this finding remains controversial. One valuable hypothesis is that brain damage and neurodegeneration is – in contrast to MS – less severe and more focal in nature in NMOSD patients. Therefore, cerebral hypometabolism seen in MS may not be a feature of NMOSD, or may be present to much lesser extent. This could potentially explain normal measures of venous density in NMOSD.

Whether, and to what extent diffuse brain damage occurs in NMOSD is a matter of controversy [21–25]. On the one hand, studies using volumetrics [23], spectroscopy [22], and diffusion tensor imaging (DTI) [24] have shown that diffuse brain atrophy in NMOSD is less pronounced than in MS, or even similar to healthy control subjects. Other studies identified widespread brain alterations in NMOSD [21, 26]. These changes were, however, less severe than in MS, which is in line with our results showing a weak trend of smaller PVA values in NMOSD versus healthy volunteers.

Venous density in NMOSD was – in contrast to MS – not associated with the number of brain lesions in our study. This discrepancy might be a consequence of more diffuse structural damage such as brain parenchymal gliosis in MS versus NMOSD, that causes decreased PVA in MS.

A limitation of this study that assessed the periventricular venous density by using a manual approach is the small sample size of the cohort respective low power in detecting subtle vascular changes. Although all images were anonymized, blinding to the MS diagnosis was not always achievable as a consequence of the existence of lesions strongly suggestive of MS. Minor motion artefacts may have also biased our results.

Despite the absence of any gender differences in PVA in healthy control subjects, we cannot exclude that gender differences between NMOSD and healthy control subjects have influenced our results.

Conclusion

In conclusion, the periventricular venous system appeared similar in NMOSD and healthy controls on 7T T2*w images. This finding is in contrast to MS and may highlight pathogenetic differences between these distinct autoimmune neuroinflammatory disease entities.

Compliance with Ethical Standards

Disclosure of potential conflicts of interest

Conflict of Interest: The authors declare that they have no conflict of interest.

Research involving Human Participants and/or Animals

All procedures performed in studies involving human participants were in accordance with the ethical standards of the institutional and/or national research committee and with the 1964 Helsinki declaration and its later amendments or comparable ethical standards.

Informed consent

Informed consent was obtained from all individual participants included in the study.

Authors' Contribution

Schumacher – Data collection and Data analysis

Pache - Data collection

Bellmann-Strobl - Data collection

Behrens - Data collection

Dusek - Project development and Data collection

Harms - Data collection

Ruprecht - Data collection

Nytrova - Data collection

Chawla - Project development

Niendorf - Project development and Data management

Kister - Project development

Paul - Project development and Data collection

Ge - Project development

Wuerfel - Project development and Data collection

Sinnecker - Project development, Data collection and Data analysis

References

1. Wingerchuk DM, Banwell B, Bennett JL, Cabre P, Carroll W, Chitnis T, de Seze J, Fujihara K, Greenberg B, Jacob A, Jarius S, Lana-Peixoto M, Levy M, Simon JH, Tenembaum S, Traboulsee AL, Waters P, Wellik KE, Weinshenker BG, International Panel for NMO Diagnosis (2015) International consensus diagnostic criteria for neuromyelitis optica spectrum disorders. *Neurology* 85:177–189.
2. Kim HJ, Paul F, Lana-Peixoto MA, Tenembaum S, Asgari N, Palace J, Klawiter EC, Sato DK, de Seze J, Wuerfel J, Banwell BL, Villoslada P, Saiz A, Fujihara K, Kim S-H, Guthy-Jackson Charitable Foundation NMO International Clinical Consortium & Biorepository (2015) MRI characteristics of neuromyelitis optica spectrum disorder: an international update. *Neurology* 84:1165–1173.
3. Jarius S, Wildemann B, Paul F (2014) Neuromyelitis optica: clinical features, immunopathogenesis and treatment. *Clin Exp Immunol* 176:149–164.
4. Kleiter I, Gahlen A, Borisow N, Fischer K, Wernecke K-D, Wegner B, Hellwig K, Pache F, Ruprecht K, Havla J, Krumbholz M, Kümpfel T, Aktas O, Hartung H-P, Ringelstein M, Geis C, Kleinschnitz C, Berthele A, Hemmer B, Angstwurm K, Stellmann J-P, Schuster S, Stangel M, Lauda F, Tumani H, Mayer C, Zeltner L, Zieman U, Linker R, Schwab M, Marziniak M, Bergh FT, Hofstadt-van Oy U, Neuhaus O, Winkelmann A, Marouf W, Faiss J, Wildemann B, Paul F, Jarius S, Trebst C, NEMOS (Neuromyelitis Optica Study Group) (2015) Neuromyelitis optica: Evaluation of 871 attacks and 1153 treatment courses. *Ann Neurol* 79:206-216.
5. Lennon VA, Kryzer TJ, Pittock SJ, Verkman AS, Hinson SR (2005) IgG marker of optic-spinal multiple sclerosis binds to the aquaporin-4 water channel. *J Exp Med* 202:473–477.

6. Paul F, Jarius S, Aktas O, Bluthner M, Bauer O, Appelhans H, Franciotta D, Bergamaschi R, Littleton E, Palace J, Seelig H-P, Hohlfeld R, Vincent A, Zipp F (2007) Antibody to aquaporin 4 in the diagnosis of neuromyelitis optica. PLoS Med 4:e133.
7. Jarius S, Ruprecht K, Wildemann B, Kuempfel T, Ringelstein M, Geis C, Kleiter I, Kleinschnitz C, Berthele A, Brettschneider J, Hellwig K, Hemmer B, Linker RA, Lauda F, Mayer CA, Tumani H, Melms A, Trebst C, Stangel M, Marziniak M, Hoffmann F, Schippling S, Faiss JH, Neuhaus O, Ettrich B, Zentner C, Guthke K, Hofstadt-van Oy U, Reuss R, Pellkofer H, Ziemann U, Kern P, Wandinger KP, Bergh FT, Boettcher T, Langel S, Liebetrau M, Rommer PS, Niehaus S, Münch C, Winkelmann A, Zettl U UK, Metz I, Veauthier C, Sieb JP, Wilke C, Hartung HP, Aktas O, Paul F (2012) Contrasting disease patterns in seropositive and seronegative neuromyelitis optica: A multicentre study of 175 patients. J Neuroinflammation 9:14.
8. Trebst C, Jarius S, Berthele A, Paul F, Schippling S, Wildemann B, Borisow N, Kleiter I, Aktas O, Kümpfel T, Neuromyelitis Optica Study Group (NEMOS) (2014) Update on the diagnosis and treatment of neuromyelitis optica: recommendations of the Neuromyelitis Optica Study Group (NEMOS). J Neurol 261:1–16.
9. Reichenbach JR, Venkatesan R, Schillinger DJ, Kido DK, Haacke EM (1997) Small vessels in the human brain: MR venography with deoxyhemoglobin as an intrinsic contrast agent. Radiology 204:272–277.
10. Tallantyre EC, Morgan PS, Dixon JE, Al-Radaideh A, Brookes MJ, Evangelou N, Morris PG (2009) A comparison of 3T and 7T in the detection of small parenchymal veins within MS lesions. Invest Radiol 44:491–494.

11. Sinnecker T, Kuchling J, Dusek P, Dörr J, Niendorf T, Paul F, Wuerfel J (2015) Ultrahigh field MRI in clinical neuroimmunology: a potential contribution to improved diagnostics and personalised disease management. EPMA J 6:16.
12. Sinnecker T, Dörr J, Pfueller CF, Harms L, Ruprecht K, Jarius S, Brück W, Niendorf T, Wuerfel J, Paul F (2012) Distinct lesion morphology at 7-T MRI differentiates neuromyelitis optica from multiple sclerosis. Neurology 79:708–714.
13. Kister I, Herbert J, Zhou Y, Ge Y (2013) Ultrahigh-Field MR (7 T) Imaging of Brain Lesions in Neuromyelitis Optica. Mult Scler Int 2013:398259.
14. Sinnecker T, Bozin I, Dörr J, Pfueller CF, Harms L, Niendorf T, Brandt AU, Paul F, Wuerfel J (2013) Periventricular venous density in multiple sclerosis is inversely associated with T2 lesion count: a 7 Tesla MRI study. Mult Scler 19:316–325.
15. Ge Y, Zohrabian VM, Osa E-O, Xu J, Jaggi H, Herbert J, Haacke EM, Grossman RI (2009) Diminished visibility of cerebral venous vasculature in multiple sclerosis by susceptibility-weighted imaging at 3.0 Tesla. J Magn Reson Imaging 29:1190–1194.
16. Polman CH, Reingold SC, Banwell B, Clanet M, Cohen JA, Filippi M, Fujihara K, Havrdova E, Hutchinson M, Kappos L, Lublin FD, Montalban X, O'Connor P, Sandberg-Wollheim M, Thompson AJ, Waubant E, Weinshenker B, Wolinsky JS (2011) Diagnostic criteria for multiple sclerosis: 2010 revisions to the McDonald criteria. Ann Neurol 69:292–302.
17. Kurtzke JF (1983) Rating neurologic impairment in multiple sclerosis: an expanded disability status scale (EDSS). Neurology 33:1444–1452.
18. Ge Y, Zhang Z, Lu H, Tang L, Jaggi H, Herbert J, Babb JS, Rusinek H, Grossman RI (2012) Characterizing brain oxygen metabolism in patients with multiple sclerosis

- with T2-relaxation-under-spin-tagging MRI. *J Cereb Blood Flow Metab Off J Int Soc Cereb Blood Flow Metab* 32:403–412.
19. Adams CW (1988) Perivascular iron deposition and other vascular damage in multiple sclerosis. *J Neurol Neurosurg Psychiatry* 51:260–265.
20. Wuerfel J, Paul F, Zipp F (2007) Cerebral blood perfusion changes in multiple sclerosis. *J Neurol Sci* 259:16–20.
21. Kimura MCG, Doring TM, Rueda FC, Tukamoto G, Gasparetto EL (2014) In vivo assessment of white matter damage in neuromyelitis optica: a diffusion tensor and diffusion kurtosis MR imaging study. *J Neurol Sci* 345:172–175.
22. Aboul-Enein F, Krssák M, Höftberger R, Prayer D, Kristoferitsch W (2010) Diffuse white matter damage is absent in neuromyelitis optica. *AJNR Am J Neuroradiol* 31:76–79.
23. Liu Y, Wang J, Daams M, Weiler F, Hahn HK, Duan Y, Huang J, Ren Z, Ye J, Dong H, Vrenken H, Wattjes MP, Shi F-D, Li K, Barkhof F (2015) Differential patterns of spinal cord and brain atrophy in NMO and MS. *Neurology* 84:1465–1472.
24. Jeantroux J, Kremer S, Lin XZ, Collongues N, Chanson J-B, Bourre B, Fleury M, Blanc F, Dietemann J-L, de Seze J (2012) Diffusion tensor imaging of normal-appearing white matter in neuromyelitis optica. *J Neuroradiol* 39:295–300.
25. Kremer S, Renard F, Achard S, Lana-Peixoto MA, Palace J, Asgari N, Klawiter EC, Tenembaum SN, Banwell B, Greenberg BM, Bennett JL, Levy M, Villoslada P, Saiz A, Fujihara K, Chan KH, Schippling S, Paul F, Kim HJ, de Seze J, Wuerfel JT, Guthy-Jackson Charitable Foundation (GJCF) Neuromyelitis Optica (NMO) International Clinical Consortium and Biorepository, Cabre P, Marignier R, Tedder T,

- van Pelt D, Broadley S, Chitnis T, Wingerchuk D, Pandit L, Leite MI, Apiwattanakul M, Kleiter I, Prayoonwiwat N, Han M, Hellwig K, van Herle K, John G, Hooper DC, Nakashima I, Sato D, Yeaman MR, Waubant E, Zamvil S, Stüve O, Aktas O, Smith TJ, Jacob A, O'Connor K (2015) Use of Advanced Magnetic Resonance Imaging Techniques in Neuromyelitis Optica Spectrum Disorder. *JAMA Neurol* 72:815–822.
26. Von Glehn F, Jarius S, Cavalcanti Lira RP, Alves Ferreira MC, von Glehn FHR, Costa E Castro SM, Beltramini GC, Bergo FP, Farias AS, Brandão CO, Wildemann B, Damasceno BP, Cendes F, Santos LMB, Yasuda CL (2014) Structural brain abnormalities are related to retinal nerve fiber layer thinning and disease duration in neuromyelitis optica spectrum disorders. *Mult Scler*. doi: 10.1177/1352458513519838

Tables and Figures

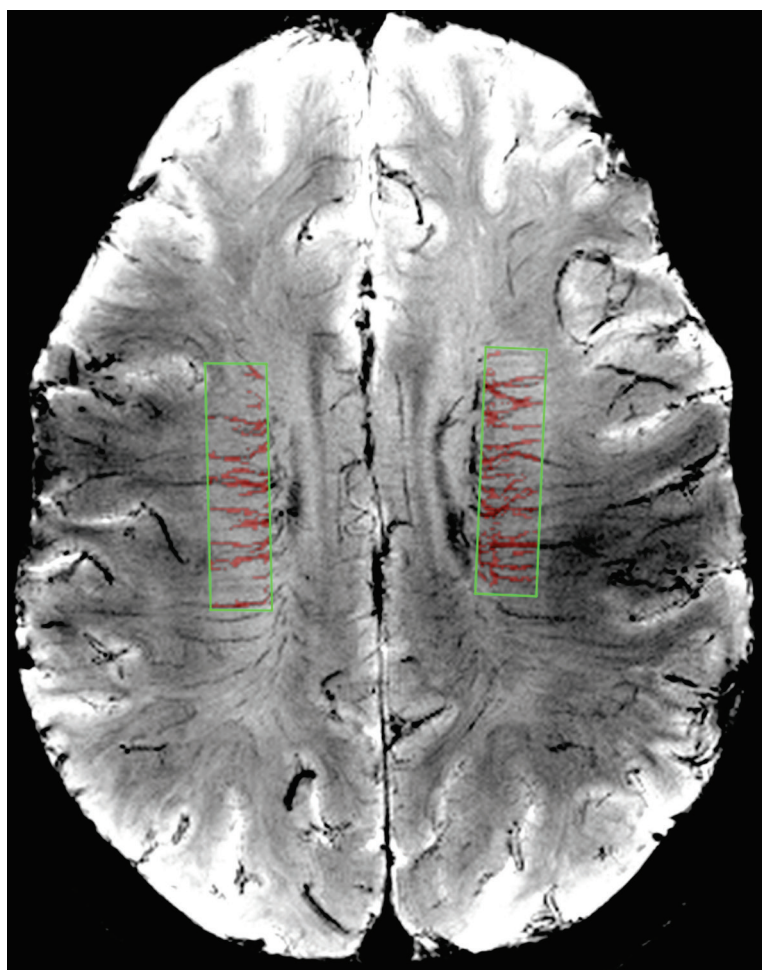


Figure 1. Method of analysis. A minimal intensity projection map of two T2*w image slices of an exemplary healthy control is presented. The blinded investigator masked each venous voxel (red area) in two squared regions of interest (ROIs, green box) as described in the methods section.

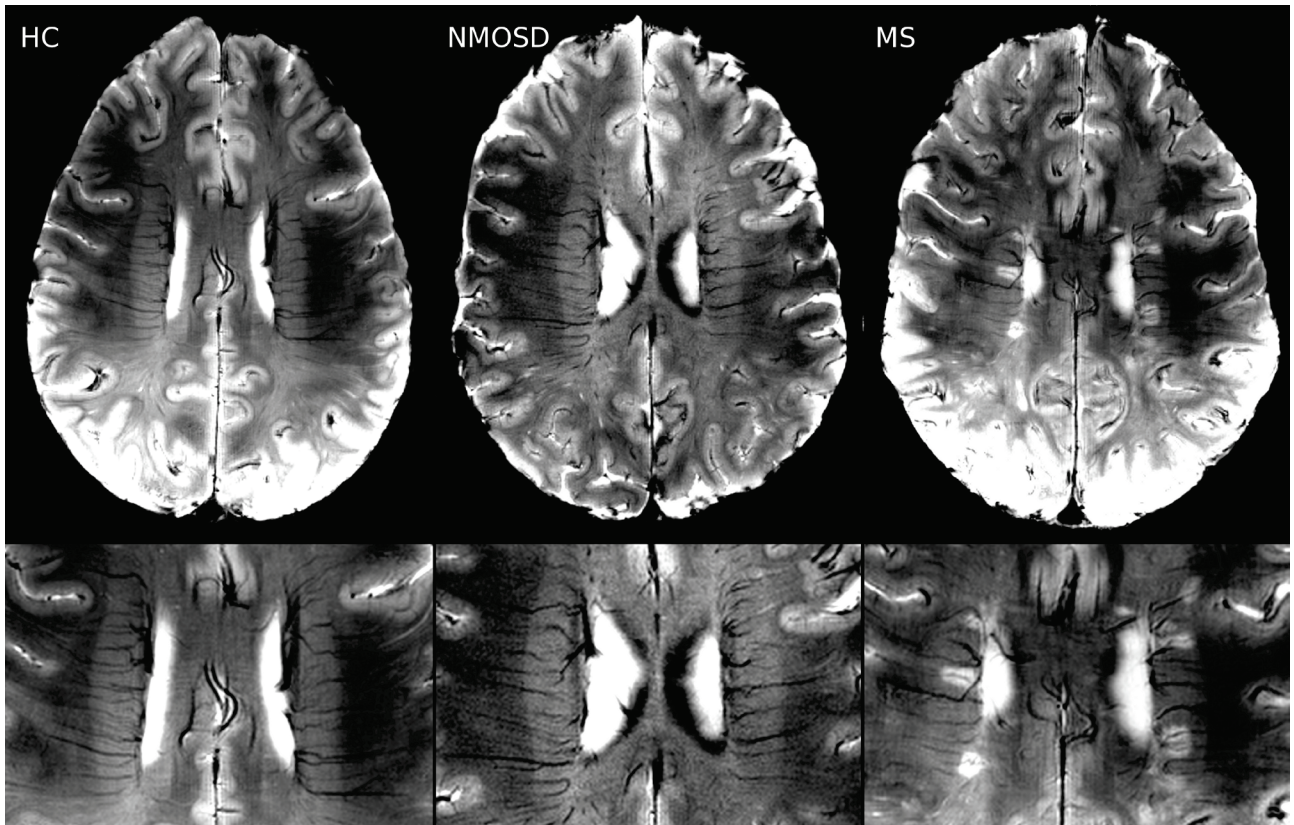


Figure 2. Periventricular venous density in a healthy control, and an exemplary NMOSD and MS patient.

7T T2*w FLASH visualizes a normal periventricular venous density in HC and NMOSD, but a moderately decreased periventricular venous vasculature in MS.

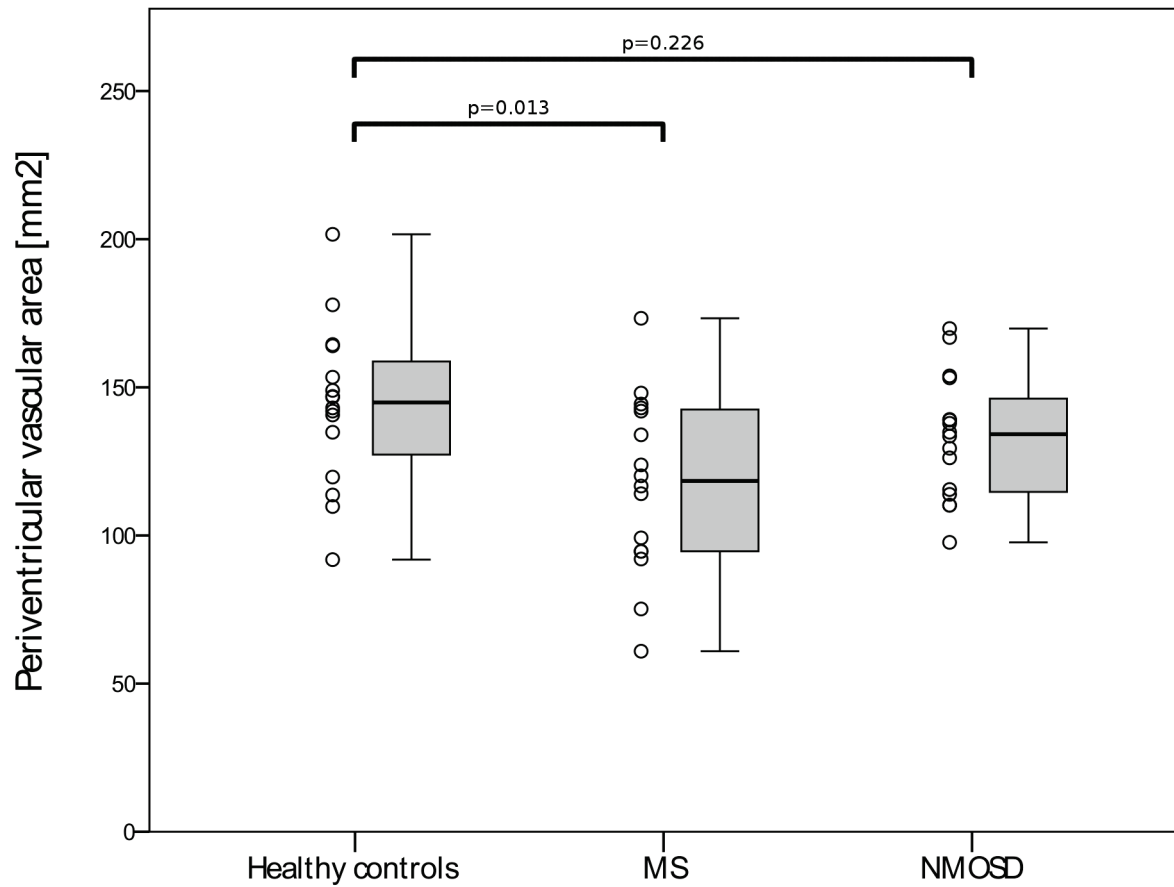


Figure 3. Plot. No statistically significant differences in periventricular venous density indicated by PVA were detectable between patients with NMOSD and healthy volunteers.

Table 1. Demographical details.

	Healthy controls	MS	NMOSD
N	16	16	16
Gender [n, female]	6	11 p=0.077 ^{&}	16 p<0.001 ^{&}
Age mean±SD, range [years]	45±15, 20-70	43±8, 26-53 p=0.608 ^{&}	48±15, 22-70 p=0.633 ^{&}
Time since first symptoms mean±SD, range [years]	-	7.5±6.9, 0.5-25.4	9.5±9.3, 1.8-34.1 p=0.515 [#]
EDSS median, range	-	1.75, 0-4.5	3.0, 1.5-6.0 p=0.086 [#]
Lesion count mean±SD, range	7±13, 0-42	22±19, 0-65 p=0.002 ^{&}	7±10, 0-38 p=0.341 ^{&}
PVA mean±SD, range [mm²]	144±27, 92-202	117±30, 61-173 p=0.013 ^{&}	133±21, 98-170 p=0.226 ^{&}

Key: PVA periventricular vascular area, [&] p-values express differences between healthy volunteers and MS or healthy volunteers and NMOSD patients. [#] p-values express differences between MS and NMOSD patients.